Journal of Biomechanics 93 (2019) 177–184

Contents lists available at ScienceDirect

Journal of Biomechanics

journal homepage: www.elsevier.com/locate/jbiomech
www.JBiomech.com

Statistical shape modelling reveals large and distinct subchondral bony differences in osteoarthritic knees

Joseph T. Lynch [a,b,*], Marco T.Y. Schneider [c], Diana M. Perriman [a,b,d], Jennie M. Scarvell [a,d], Mark R. Pickering [e], Md. Asikuzzaman [e], Catherine R. Galvin [a,b], Thor F. Besier [c], Paul N. Smith [a,b]

[a] Australian National University, Australia
[b] Trauma and Orthopaedic Research Unit, Canberra Hospital and Health Services, Australia
[c] Auckland Bioengineering Institute, University of Auckland, New Zealand
[d] University of Canberra, Australia
[e] School of Engineering and Information Technology, University of New South Wales, Canberra, Australia

ARTICLE INFO

Article history:
Accepted 2 July 2019

Keywords:
Osteoarthritis
Knee
Statistical shape model

ABSTRACT

Knee osteoarthritis (OA) results in changes such as joint-space narrowing and osteophyte formation. Radiographic classification systems group patients by the presence or absence of these gross anatomical features but are poorly correlated to function. Statistical-shape modelling (SSM) can detect subtle differences in 3D-bone geometry, providing an opportunity for accurate predictive models. The aim of this study was to describe and quantify the main modes of shape variation which distinguish end-stage OA from asymptomatic knees. Seventy-six patients with OA and 77 control participants received a CT of their knee. 3D models of the joint were created by manual segmentation. A template mesh was fitted to all meshes and rigidly aligned resulting in a set of correspondent meshes. Principal Component Analysis (PCA) was performed to create the SSM. Logistic regression was performed on the PCA weights to distinguish morphological features of the two groups. The first 7 modes of the SSM captured >90% shape variation with 6 modes best distinguishing between OA and asymptomatic knees. OA knees displayed subchondral bone expansion particularly in the condyles and posterior medial tibial plateau of up to 10 mm. The model classified the two groups with 95% accuracy, 96% sensitivity, 94% specificity, and 97% AUC. There were distinct features which differentiated OA from asymptomatic knees. Further research will elucidate how magnitude and location of shape changes in the knee influence clinical and functional outcomes.

1. Introduction

Osteoarthritis (OA) is a disease that involves the breakdown of cartilage and underlying bone resulting in pain and altered joint dysfunction (Arthritis Australia, 2014; Australian Commission on Safety and Quality in Health Care, 2017). In Australia, OA is estimated to affect 8.1% (over 2 million) of the population and costs Australia over $3.2 billion per year (Arthritis Australia, 2014). The response to this disease has been an increase in total knee replacement (TKR) which, given the projected increase in average population age and obesity, is likely to become financially unsustainable (Abhishek and Doherty, 2013). Outcomes of TKR are variable, with up to 20% of patients reporting dissatisfaction following their operation (Bourne et al., 2010). Therefore, the importance of deepening our understanding of OA and the role of joint replacement versus other interventions in disease progression and amelioration has become more urgent.

Bony knee shape is changed in OA but clinical imaging data is not well correlated with pain and function (Barr et al., 2015). The clinical diagnosis of osteoarthritis can be made from the history, symptoms and signs alone (Abhishek and Doherty, 2013), but the severity of the disease is commonly determined from visualising tissue morphologic changes on imaging (Van Manen, Nace and Mont, 2012). Bone is normally imaged with 2D plain x-ray (Kellgren and Lawrence, 1957) or computed tomography (CT) (Chan et al., 1991) while Magnetic Resonance Imaging (MRI) is also

* Corresponding author at: The Trauma and Orthopaedic Research Unit, Building 6, Level 1, The Canberra Hospital, Garran, ACT, Australia.
E-mail addresses: Joseph.lynch@anu.edu.au (J.T. Lynch), msch153@aucklanduni.ac.nz (M.T.Y. Schneider), diana.perriman@anu.edu.au (D.M. Perriman), jennie.scarvell@canberra.edu.au (J.M. Scarvell), m.pickering@unsw.edu.au (M.R. Pickering), m.asikuzzaman@unsw.edu.au (Md. Asikuzzaman), catherine.galvin@anu.edu.au (C.R. Galvin), t.besier@auckland.ac.nz (T.F. Besier), psmith.admin@orthoact.com.au (P.N. Smith).

https://doi.org/10.1016/j.jbiomech.2019.07.003
0021-9290/

used to help clinicians assess soft tissue damage and further understand the degree of disease severity (Hunter et al., 2011). The appearance of an osteoarthritic knee is highly variable with differing amounts of condylar squaring (Fairbank, 1948), tibial flattening and widening (Ding, Cicuttini and Jones, 2007), joint space narrowing, and osteophyte formation (Kellgren and Lawrence, 1957). These changes give each osteoarthritic knee its own unique bony shape. However, people with OA knee present with different levels of pain and functional limitation regardless of their imaging findings (Hunter et al., 2013). It is probable that simple visual inspection of clinical imaging is insufficient to detect the subtle changes associated with pain and dysfunction. Advancements in both medical imaging and computational modelling allow for analysis of the entire shape of joints in a way that clinical imaging assessments cannot. These techniques offer an avenue for objectively classifying shape due to OA in order to evaluate associations with symptoms and progression.

Statistical Shape Modelling (SSM) precisely characterises complex shapes by grouping coincident shape parameters using Principal Component Analysis (PCA). PCA decomposes shapes into a set of discrete components, or modes, which describes the main ways in which the shape varies across the population (Cootes et al., 1992; Dryden and Mardia, 1998). The modes can then be compared to detect what shape features are different between cohorts (Agricola et al., 2015; Schneider et al., 2015, 2018; Pavlova et al., 2017). Additionally, SSM allows for the analysis of specific associations between regional anatomy and parameters such as kinematics and joint contact mechanics (Schneider et al., 2017), which are known to be affected by OA. This method differs from current clinical measurement strategies because it is not limited by *a priori* assumptions and systems. Instead, the patterns and relationships are permitted to emerge from the data. In this way associations between shape and other important determinants of function and wellness can be interrogated.

Bone shape has been found to differentiate between OA and healthy knees, but 3D regional anatomical differences have not been systematically explored. Research describing changes in the knee using SSM have identified whole joint subchondral boneshape as a possible biomarker for differentiating between healthy and osteoarthritic knees (Bredbenner et al., 2010; Haverkamp et al., 2011; Neogi et al., 2013; Barr et al., 2016). Bredbenner et al. conducted a landmark study using a longitudinal image database which demonstrated that people with OA knees had observable shape characteristics prior to symptom development. These included a slight expansion of the posterior and distal condylar surfaces and spreading and depression of the tibial plateau. Further, Bredbenner et al. quantified the magnitude of these changes using SSM. This study was crucial because it demonstrated that shape is an important factor in the development of OA. Other researchers have proceeded to identify specific shape characteristics of symptomatic OA knees. Specifically, the femur displays widening and flattening of the femoral condyle, expansion around the cartilage plate and narrowing of the intercondylar notch (Neogi et al., 2013; Bowes et al., 2015; Barr et al., 2016). The tibia is described as having an "elevated" lateral plateau, a reduction in the space between tibial spines and increase in bone area most prominent along the perimeter of the bone (Haverkamp et al., 2011; Bowes et al., 2015). Although the tibia has been described as undergoing uniform changes in OA (Barr et al., 2016), these claims are apparently unsubstantiated with actual data. While we know that bony shape differentiates the OA knee from the asymptomatic knee (Shepstone et al., 2001; Haverkamp et al., 2011; Neogi, 2012; Neogi et al., 2013; Barr et al., 2016), we don't yet know which regional anatomic features are the most important when differentiating end-stage OA from asymptomatic. Nor do we know the magnitude of these changes. Therefore, the aim of this study was to describe and quantify the main modes of shape variation which distinguish end-stage OA from age- and sex-similar asymptomatic knees.

2. Methods

2.1. Participants

The participants in this study were recruited as part of a larger randomised controlled trial of knee replacement designs with age- and sex-similar asymptomatic control participants (ISRCTN75076749). The OA group included 76 patients who were awaiting TKR for OA. The asymptomatic group (N = 77) were included if they were pain free with no history of lower limb pathology. Participants included 52% and 56% females in the asymptomatic and OA group, respectively and were similar in age (mean 67.6 and 66.8 years, respectively) (Table 1). All participants provided written consent and ethics approval was granted by the Australian Capital Territory Health and the Australian National University human research ethics committees.

2.2. Data collection

Participants received a 3D-spiral CT scan (Toshiba Medical Systems, Ōtawara, Japan) of the knee with a field of view of at least 150 mm above and below the tibiofemoral joint line. The OA knees were selected based on which knee was being operated on. If the surgery was a bilateral TKR, then the participant selected their worst knee. The side used in the asymptomatic group was matched to the OA group. Slice thickness was 1 mm with a resolution of 512×512 voxels with spatial dimensions $0.625 \times 0.625 \times 0.5\ mm^3$ and 16 bits/pixel.

2.3. Image processing

The femur and tibia were isolated from the CT scan images by manual segmentation using custom software (Orthovis v4 Matlab, The Mathworks, Inc., Natick, MA). Manual segmentation is more precise that automatic because it allows the operator to include individual features like osteophytes. Intra- and inter-rater variations of the calculated volumes for the femur were 0.99 and 0.84, and for the tibia 0.98 and 0.77 respectively. Three-dimensional coordinate systems for the femur and tibia were established using standard referencing convention defined by Grood and Suntay (Grood and Suntay, 1983). Orthogonal references frames were established based on individual anatomical locations for each tibia and femur in the dataset. Origins were set for the femur at the most proximal point of the intercondylar notch and, for the tibia, at the mid-point of the tibial spines.

Following axis selection, each model was cropped to allow proportional sizing. Using the anterior/posterior projection of the CT, the femur was cropped at 1.5X the distance from the distal femoral

Table 1
Patient demographics.

Participant characteristics	Asymptomatic	OA
N	77	76
Age (years)	67.6 ± 10.81	66.8 ± 9.17
Number of females (%)	40 (52%)	43 (56%)
Left Sided Knees (% L)	36 (47%)	36 (47%)
N by KL Grade: 0-1-2–3-4	35-30-9-3-1	0-0-1-23-52
Height (cm)	167.8 ± 9.73	169.3 ± 9.74
Weight (kg)	70.2 ± 12.78	89.2 ± 19.04
BMI (kg m^2)	24.9 ± 3.85	31.0 ± 5.37

Note. KL – Kellgren Lawrence grade; BMI – Body Mass Index.

condyles to the adductor tubercle. The tibia was cropped 1.5X the distance from the most proximal aspect of the tibial spine to the most inferior point of the superior tibiofibular joint (Fig. 1). Corresponding femurs and tibias were recombined using a custom Matlab script to create a tibiofemoral joint for each participant. The tibia and femur were not considered separately because of their shape co-dependence. Variations in alignment were controlled for by aligning the femur and tibial meshes so that their axes were orientated at zero degrees of rotation and translation. The 3D models were exported as meshed surfaces. Knee models were down sampled to 30,000 vertices, and smoothed using a Laplacian filter (MeshLab 2016.12, http://meshlab.sourceforge.net). For consistency, left-side meshes were mirrored so they appeared as right-sided. These combined tibiofemoral meshes were used in the SSM for consistency. Meshes from both osteoarthritic and asymptomatic groups were combined in order to create one SSM.

2.4. Statistical shape model generation

The technique implemented for this study was based on previous methods (Zhang et al., 2014; Schneider et al., 2015). Firstly, a template mesh was created using a series of radial basis functions to parameterise the tibiofemoral joint (Zhang, Ackland and Fernandez, 2018). This template was based on a single mesh from one knee in the dataset. This template was iteratively fit with a series of coarse to fine fits to all meshes in the dataset, which resulted in maximum correspondence between meshes. Corresponding meshes were then rigidly aligned, using a partial Procrustes analysis which minimised the least-squared distances of corresponding points (Gower, 1975). This allowed for only the shape and scaling variability to be included in the model.

Principal Component Analysis (PCA) was then run on the nodal coordinates of the aligned meshes to create a shape model. PCA is used for dimension reduction which allows any shape in the data set x to be approximated as the sum of the mean shape $\bar{x}$ plus the weighted sum of the principal components ϕ (Heimann and Meinzer, 2009; Schneider et al., 2015):

$$x = \bar{x} + \sum_{i=0}^{n} \omega_1 \phi_1$$

where n is the number of principal components needed to explain 90% of the total variation in the population. Therefore, the shape of each bone was described by n principal component (PC) weights, ω, where ω are the amount of variation along an individual principal component.

Following visual inspection of each mesh to ensure the basic shape was correct, the fitting process was repeated using the mean shape as the template. Following this, the fitting process was further refined for individual shape differences by incorporating PCA fitting using the previous statistical shape model generated from the dataset. In this way, the shape model was optimised by propagating fitting correspondence across the dataset to a RMS error of 0.89 mm. A final PCA was performed to generate a statistical shape model which generated the PC weights used in the subsequent analysis. The tibiofemoral PC weights were extracted for each subject from each shape model for logistic regression. Mode weights were normalised to z-scores for consistency and outliers were truncated to 2.5 SD.

2.5. Statistics

Binary logistic regression modelling was used to determine the shape parameters which best discriminated between OA and asymptomatic knees (SPSS v25, SPSS Inc., Chicago, Illinois). The model included BMI, gender and age. The model added principal components in a stepwise fashion until there was no more statistically significant improvement of the fit of the model. Principal components which best distinguished between OA and asymptomatic shapes, along with their corresponding coefficients and odds ratios, were reported. Pointwise distances were calculated and visualised to compare anatomical differences between the reconstructed mean-OA and mean-asymptomatic knees. Furthermore, pointwise distances were also calculated for the reconstructed principal components which best distinguished between OA and asymptomatic. These differences were reported as plus and minus 2 standard deviations away from the mean shape and expressed in millimetres (mm) and percentages in order to quantify the differences between OA and asymptomatic for the entire population.

The effectiveness of the SSM to distinguish between OA and asymptomatic knees was evaluated using a leave-one-out cross validation to generate area under the receiver operator characteristic (ROC) curve (AUC), with sensitivity, specificity, classification accuracy, and positive and negative likelihood ratio (IBM SPSS Modeller for Windows, version 18.2, IBM Corp., Armonk, N.Y., USA).

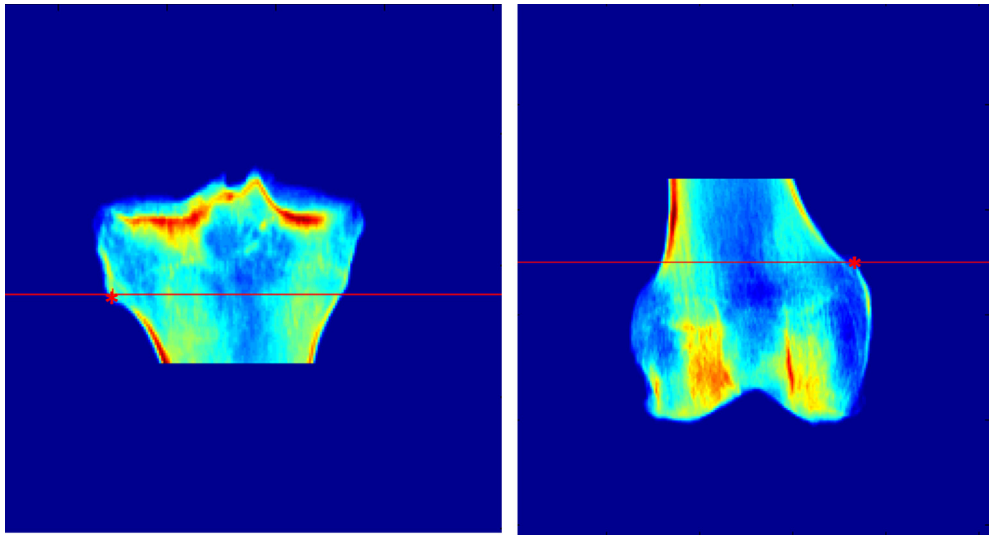

Fig. 1. Cropping locations for femur and tibia. The tibia was cropped at the superior tibiofibular joint (*) and the femur was cropped at the adductor tubercle (*).

3. Results

The first seven principal components of the combined end-stage OA and asymptomatic SSM accounted for 90% of the total variance in knee joint morphology (Fig. 2). The variation explained in the entire model by each mode ranged from 77.04% for mode one to 1.23% for mode 7. As expected, since we did not control for scaling, mode one explained the isometric sizing component of the model (Bredbenner et al., 2010; Schneider et al., 2018).

Logistic regression results showed that a combination of BMI and 4 modes of variation significantly distinguished between OA and asymptomatic joints ($p < 0.05$). Table 2 describes the odds ratios for significant predictors. The model displayed a leave-one-out accuracy of 94.8%, 96.0% sensitivity, 93.7% specificity, 97.0 area under ROC curve, 15.16 positive-likelihood ratio, and 0.04 negative-likelihood ratio.

A comparison of the mean differences between OA and asymptomatic knees provided a summary of the modal differences. These included expansion of the femoral cartilage plate extending anteriorly, medially and laterally (Fig. 3). Posteriorly, there was a large area of bony expansion on the proximal femoral condyle approximately, which equated to an increase of approximately 5 mm (115%)in height compared to asymptomatic knees. On the tibial surface, both medial and lateral plateaus appeared slightly depressed and there was an area of bony expansion on the medial aspect of the tibia extending posteriorly and finishing in a tubercle on the posterior medial plateau which was 3 mm larger in the OA knee compared to asymptomatic.

Mode 2 described 3.48% of the anatomical variation within the model. Visually, this component represented large regional differences in the anterior femoral cartilage plate extending posteriorly along the medial and lateral borders (Fig. 4c). Posteriorly, this mode described an area of bony expansion on the medial condyle resulting in a reduced intercondylar fossa (Fig. 4d). Tibial differences included expansion of the posterior-medial aspect of the tibial border, causing narrowing of the posterior intercondylar fossa (Fig. 4b). Finally, mode 2 described a region of expansion within the proximal tibiofibular joint (Fig. 4a).

Mode 5 explained 1.64% of the anatomical variation and described changes in the height of the tibial plateau and spines (Fig. 5a); and a region of large bony expansion on the proximal aspect of the posterior medial condyle which differed 10 mm from asymptomatic femurs (Fig. 5b).

Mode 6 (1.45% explained variance) described unique bony shape differences between OA and asymptomatic knees. Specifically, the most prominent feature was a tubercle on the perimeter of the posterior medial tibial plateau (Fig. 5c). Further differences were detected within the medial femoral cartilage plate and on the medial aspect of the lateral femoral condyle (Fig. 5d).

4. Discussion

The purpose of this study was to identify unique bony shape features which distinguish between end-stage OA and asymptomatic knees using statistical shape modelling (SSM). This is the first study to quantify the extent of the bony changes which occur

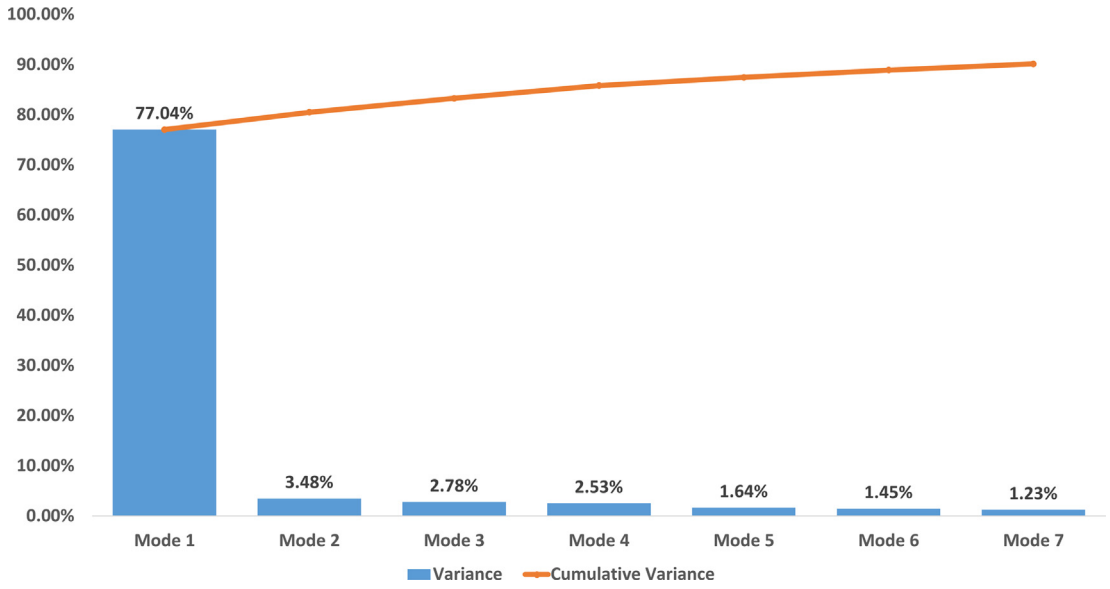

Fig. 2. Individual and Cumulative variation explained by the statistical shape model.

Table 2
Logistic Regression output – modes of shape variation which significantly differentiate OA from asymptomatic groups.

	Mean ± Standard Deviation					
	Asymptomatic (n = 77)	OA (n = 76)	Coefficient	OR (95% CI)	Sig	Outliers
BMI	24.9 ± 3.85	31.0 ± 5.37	0.42	1.5 (1.1, 2.0)	0.01	5
Mode 1	−0.22 ± 0.92	0.23 ± 1.04	2.39	10.9 (2.2, 53.1)	0.00	4
Mode 2	−0.49 ± 0.68	0.49 ± 1.03	6.01	405.8 (14.7, 11205.3)	0.00	4
Mode 5	−0.42 ± 0.82	0.43 ± 0.99	4.69	108.9 (7.6, 1554.7)	0.00	4
Mode 6	−0.34 ± 0.79	0.34 ± 1.07	4.24	69.2 (5.6, 860.0)	0.00	3
Constant	–	–	−9.58	–	0.02	–

Note. OR = odds ratio; CI = confidence interval; Sig = p values of individual predictors.

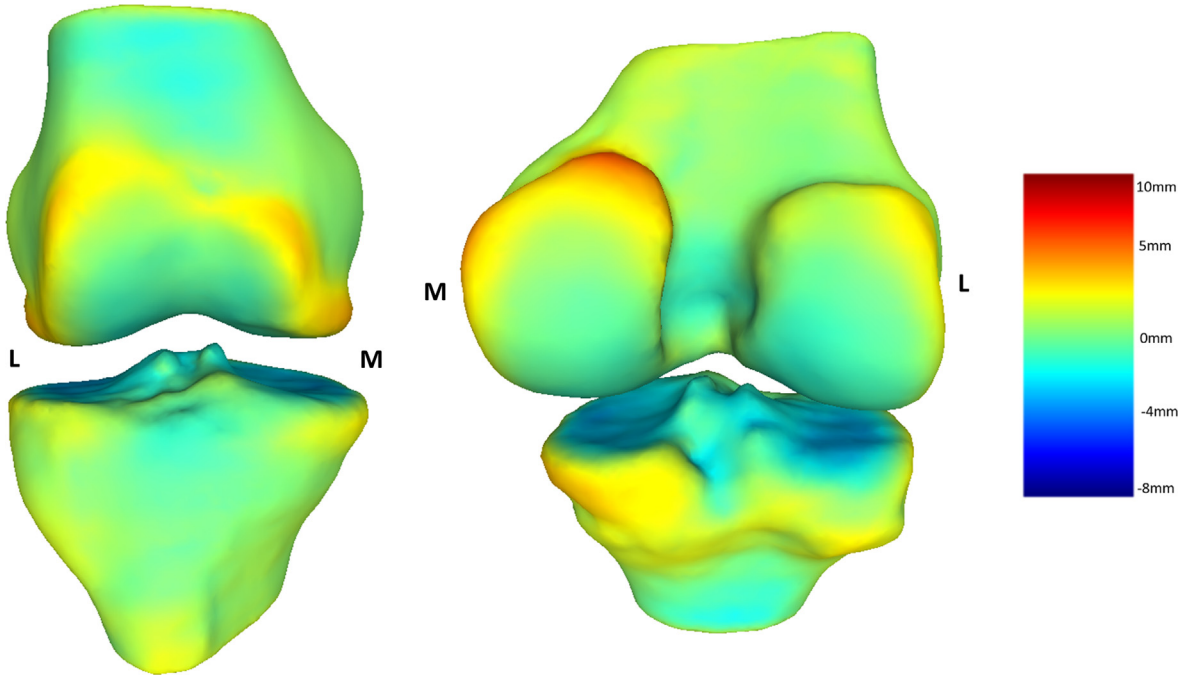

Fig. 3. Pointwise differences in surface geometry of the reconstructed mean-OA knee relative to mean-asymptomatic knees. Left: anterior view; right: posterior-superior view. Knees displayed as right sided. Heat map indicates the extent of the variation in the local anatomy. M = Medial; L = Lateral.

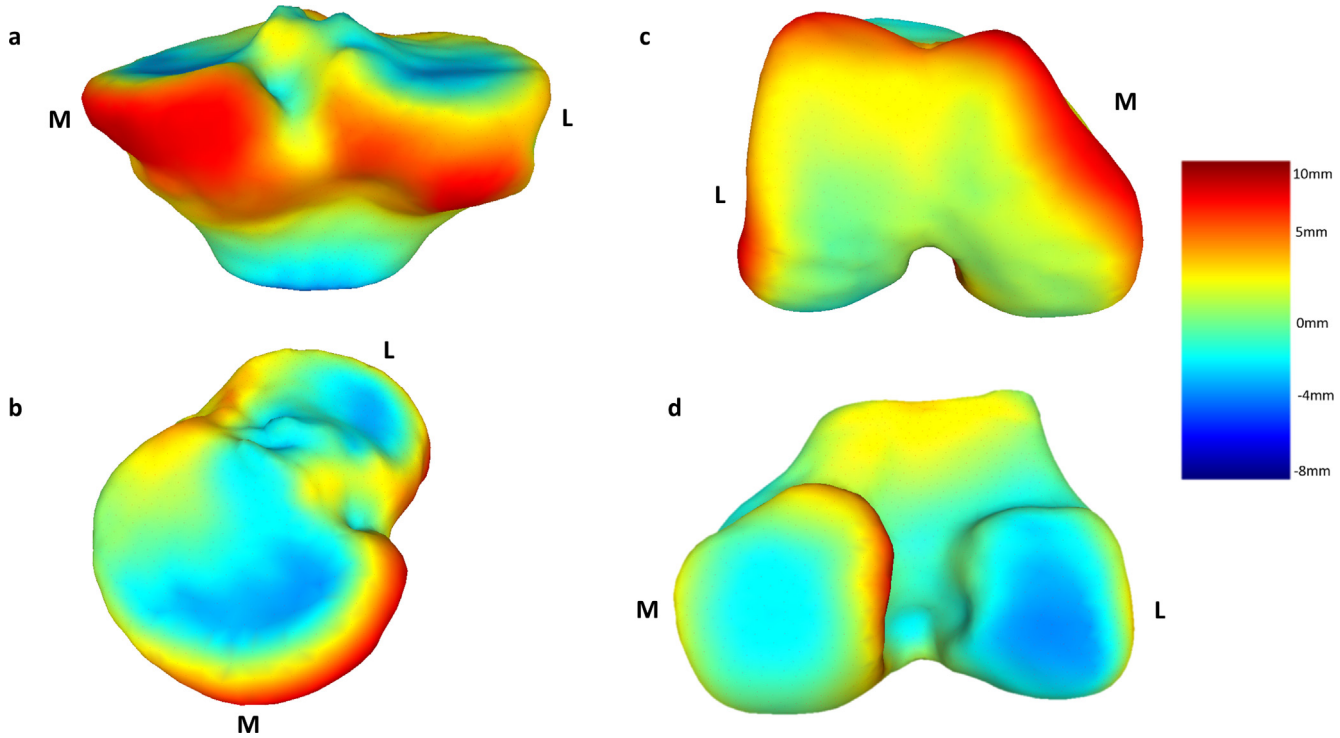

Fig. 4. Pointwise differences in surface geometry of OA knees relative to asymptomatic knees using mode 2 weightings. (a) posterior view of tibia; (b) anterior medial view of tibia; (c) femoral articular surface view; (d) posterior view of femur. Heat map indicates the extent of the variation in the local anatomy measured at plus and minus two standard deviations away from the mean shape for the population. M = Medial; L = Lateral.

in end-stage OA knee. The main finding was that OA knees displayed bony expansion at the edges of the OA tibial and femoral cartilage plates which were up to 10 mm (190%) larger than asymptomatic controls (Fig. 4). Furthermore, we found a posteromedial tibial tubercle that was 6 mm (115%) larger than asymptomatic tibias (Fig. 5c) with a corresponding posterior-medial condylar expansion which was up to 10 mm (190%) larger than asymptomatic femurs (Fig. 5b). This may explain the difficulty people with OA knee have in achieving full flexion. Additionally, we found that shape features captured by the model could distinguish between asymptomatic and OA knee shapes with an accuracy of 94.8%. Finally, combining the shape model with logistic regression

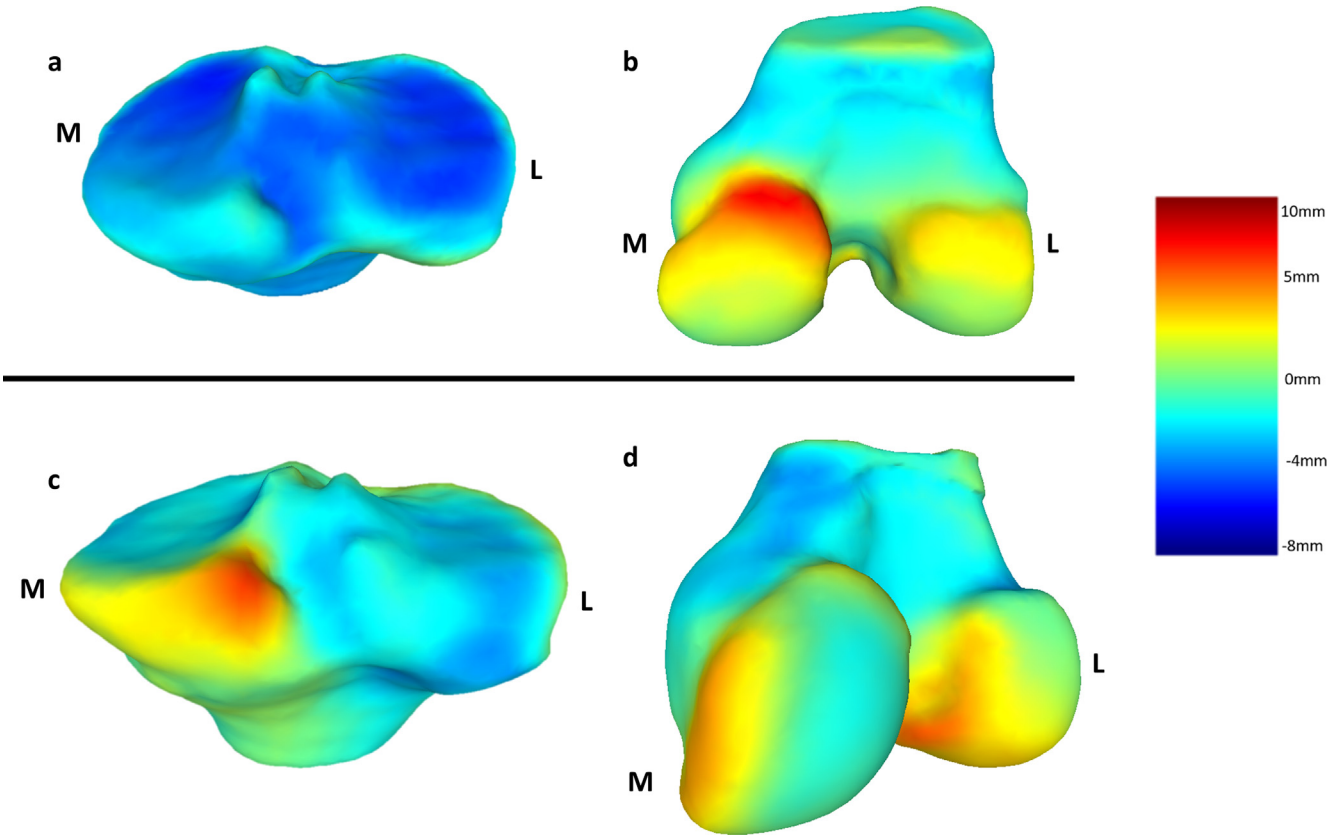

Fig. 5. Pointwise differences in surface geometry of OA knees relative to asymptomatic knees for mode 5 (upper) and mode 6 (lower). (a) posterior view of tibia; (b) posterior femur; (c) posterior view of tibia; (d) posterior-medial view of femur. Knees displayed as right sided. Heat map indicates the extent of the variation in the local anatomy measured at plus and minus two standard deviations away from the mean shape for the population. M = Medial; L = Lateral.

allowed for the identification of the different shape arrays which characterise OA knees.

There are a number of femoral features which distinguish OA from asymptomatic shapes. These features are regions of bony expansion, with pointwise differences of up to 10 mm (190%), extending throughout the femoral cartilage plate and the femoral borders. Specifically, these changes were the greatest anteriorly, medially, and on the proximal aspect of the posterior-medial condyle. While these changes are similar to those reported in the literature, our study is the first to quantify the potential extent of bony expansion between OA and asymptomatic knees (Neogi et al., 2013; Bowes et al., 2015; Barr et al., 2016). Additionally, there is reduced space within the intercondylar notch which is caused by the expansion of the bone on the medial and lateral condyles of the femur. Several studies have reported similar changes to the intercondylar notch in OA knees noting the increased presence of osteophytes seen on MRI (Shepstone et al., 2001; Chen et al., 2016; Sasho et al., 2017). Flattening of the posterior femoral condyles, particularly the lateral condyle, was observed indicating increased levels of bone remodelling (Matsuda et al., 2004). Therefore, the distal femur in our OA cohort was characterised by significant cartilage plate expansion, a reduced intercondylar notch and flattened condyles.

The tibia demonstrated its own distinct pattern of osteoarthritic changes. Mode 6 describes a large bony tubercle on the posterior-medial plateau of the osteoarthritic tibia which deviates by up to 6 mm (115%) larger than asymptomatic knees. This tubercle has been reported only once previously when Neogi observed it as part of an SSM but did not comment on its significance (Neogi et al., 2013). The fact that it is not commonly reported in relation to OA knee shape is perplexing but may be due to it being occluded on 2D x-ray or missed in MRI slice selection. This tubercle appears to lie under the posterior horn of the medial meniscus. The meniscus is regularly reported as torn in patients undergoing a TKR and the subchondral-bone changes are possibly a result of increased levels of contact stresses which are seen in the medial compartment (Thambyah, Goh and De, 2005). Modes 2 and 5 describe changes to the anterior, medial, and posterior borders of the proximal tibia. Previous studies report an overall increase in cross-sectional area of an osteoarthritic tibial plateau (Wang, Wluka and Cicuttini, 2005; Wluka et al., 2005; Barr et al., 2014). Our study provides much more specific data and indicates that the expansion is not in the overall size, but is caused by some distinct regional changes.

The parameter within the model which explained the most variation in the SSM was mode 1 and was knee size. Additionally, OA knees were slightly larger than asymptomatic. This finding has been described previously where OA knee size was found to significantly increase over 12 months (Hudelmaier and Wirth, 2016). The authors suggested that increased BMI might be the driver for this increase in knee size. BMI was also a significant distinguishing factor in our model. This was expected due to the fact that the OA group was heavier and increased weight is a known risk factor for knee OA. Although we don't understand the reason for the relative increase in size in the OA group given that osteophytic changes aren't captured in this mode, it is possible that the increase in size is a result of the difference in BMI between the groups.

The interplay between femoral and tibial geometry may play a role in tibiofemoral kinematics (Freeman and Pinskerova, 2005; Pinskerova et al., 2009; Smoger et al., 2015). Osteoarthritis changes kinematics, specifically femoral roll back and the loss of terminal flexion (Scarvell et al., 2018). There are corresponding areas within

the posterior femur and tibia which impinge during deep flexion in normal knees (Yildirim et al., 2007). In OA knees, limited flexion and difficulty kneeling is common (Steultjens et al., 2000). In this study, the bony expansion on the proximal aspect of the posterior medial condyle combined with the tubercle on the posterior medial tibia may be the cause of premature bony contact and loss of deep flexion in OA. Another common kinematic alteration in OA is increased knee varus thrust during gait (Foroughi, Smith and Vanwanseele, 2009; Bytyqi et al., 2014). The cartilage plate expansion observed on the medial aspects of the femur and tibia are likely to be associated with varus thrust and the altered loading environment that occurs during OA (Brand and Claes, 1989; Isaacson and Brotto, 2014). The findings of this study will allow the examination of the associations between specific shape changes and functional deficits. These analyses have not previously been performed.

The ability of SSM to discriminate the gross and subtle geometric differences between OA and asymptomatic knees potentially make it an effective predictive and diagnostic tool. Effective clinical decision making with respect to when operative intervention is appropriate is an imprecise art. TKR are increasingly being performed but there is an appetite to exhaust other measures prior to this definitive treatment. SSM offers the opportunity for identification of OA features, monitoring progression, and response to therapies. This concept has been proposed previously by Bredbenner et al. They identified subtle features in knees which proceeded to OA compared to those that didn't (Bredbenner et al., 2010). The features included a slight expansion of the posterior and distal condylar surfaces and spreading and depression of the tibial plateau. We found more tangible and extensive differences, for example expansions of up to 10 mm (190%) around the cartilage plates and the development of tibial tubercle of which was up to 6 mm (115%) in size. These findings may be important in discriminating between patients who may respond favourably to rehabilitation programs and those who do not. End-stage OA implies awaiting a knee replacement and yet there are non-surgical strategies for ameliorating knee pain in severe OA knee (Skou et al., 2015). Skou et al. demonstrated that 25% of patients removed themselves from the waiting list following a strengthening and education program. It is possible that the 25% did not demonstrate such extensive change in particular features making them more amenable to non-surgical treatment. Clearly this requires further investigation. Therefore, the data presented in this study further advances our understanding about the bony changes that occur in the osteoarthritic knee.

The results of this study should be interpreted in the light of its limitations. The cohorts included were distinctly different. One group had no knee symptoms and the other included people awaiting knee replacement. Although there was variation in terms of Kellgren-Lawrence (KL) grade within each group, the middle grades (2 and 3) were sparsely populated (Table 1). Although the polarity of the participants was useful in illustrating the degree of the shape deviation in OA, future studies would benefit from analyzing the shape deviations across the OA spectrum. The asymptomatic group contained 4 participants who had radiographic OA. However, we were interested in the shape of asymptomatic knees versus OA. An interesting future study might be to examine the differences between symptomatic vs asymptomatic OA. We did not include the patella in this study and it is possible that patella shape may have influenced the shape changes in the trochlear region of the femur. Finally, individual patient-specific osteophytes are likely not included in these analyses due to their heterogeneous nature. Since the SSM captures areas of high variability in descending order, the osteophytes will only appear in the lower order modes where the variation is very small (<1% explained).

In conclusion, the novel contribution of this study lies in the identification and quantification of the changes that occur in knees due to OA. Shape changes in osteoarthritic and asymptomatic knees were accurately captured and classified with 7 modes of variation. Using logistic regression, unique shape arrays differentiated OA from asymptomatic knees. The shape variation models described may provide a sensitive predictive tool for use in surgical and non-surgical decision making. Further studies will elucidate how the knee shape arrays identified in this study influence the disability related to knee OA.

Role of the funding source

This work was supported by ZimmerBiomet as well as the Australian Government Research Training Program (AGRTP).

Declaration of Competing Interest

The authors declare that we have no financial or personal relationships with other people or organizations that could inappropriately influence (bias) our work.

References

Abhishek, A., Doherty, M., 2013. Diagnosis and Clinical Presentation of Osteoarthritis. Rheum. Dis. Clin. North Am. 39 (1), 45–66.
Agricola, R., Leyland, K.M., Bierma-zeinstra, S.M.A., Thomas, G.E., Emans, P.J., Spector, T.D., Weinans, H., Waarsing, J.H., Arden, N.K., 2015. Validation of statistical shape modelling to predict hip osteoarthritis in females: data from two prospective cohort studies (Cohort Hip and Cohort Knee and Chingford). Rheumatology 54 (54), 2033–2041.
Arthritis Australia. (2014). Time to Move: Osteoarthritis A national strategy to reduce a costly burden TIME TO MOVE: ARTHRITIS. Broadway, NSW. Available at: http://www.arthritisaustralia.com.au/images/stories/documents/reports/TTM/Final Arthritis Aus Time to Move_OA_140618.pdf (accessed: 16 January 2018).
Australian Commission on Safety and Quality in Health Care. (2017). Osteoarthritis of the Knee: Clinical Care Standard. Sydney.
Barr, A., Dube, B., Hensor, E.M.A., Kingsbury, S.R., Peat, G., Bowes, M.A., Sharples, L.D., Conaghan, P.G., 2016. The relationship between three-dimensional knee MRI bone shape and total knee replacement—a case control study: data from the Osteoarthritis Initiative. Rheumatology 55 (May), 1585–1593.
Barr, A.J., Campbell, M.T., Hopkinson, D., Kingsbury, S.R., Bowes, M.A., Conaghan, P. G., 2015. A systematic review of the relationship between subchondral bone features, pain and structural pathology in peripheral joint osteoarthritis. Arth. Res. Ther. 17 (1), 228.
Barr, A.J., Dube, B., Hensor, E.M.A., Kingsbury, S.R., Peat, G., Bowes, M.A., Conaghan, P.G., 2014. The relationship between clinical characteristics, radiographic osteoarthritis and 3D bone area: data from the Osteoarthritis Initiative. Osteoarth. Cartil. 22, 1703–1709.
Bourne, R.B., Chesworth, B.M., Davis, A.M., Mahomed, N.N., Charron, K.D., 2010. Patient Satisfaction after Total Knee Arthroplasty: Who is Satisfied and Who is Not? Clin. Orthop. Relat. Res.? 468 (1), 57–63
Bowes, M.A., Vincent, G.R., Wolstenholme, C.B., Conaghan, P.G., 2015. A novel method for bone area measurement provides new insights into osteoarthritis and its progression. Ann. Rheum. Dis. 74 (3), 519–525.
Brand, R., Claes, L., 1989. The law of bone remodelling. J. Biomech. 22 (2), 185–187.
Bredbenner, T.L., Eliason, T.D., Potter, R.S., Mason, R.L., Havill, L.M., Nicolella, D.P., 2010. Statistical shape modeling describes variation in tibia and femur surface geometry between Control and Incidence groups from the Osteoarthritis Initiative database. J. Biomech. 43, 1780–1786.
Bytyqi, D., Shabani, B., Lustig, S., Cheze, L., Karahoda Gjurgjeala, N., Neyret, P., 2014. Gait knee kinematic alterations in medial osteoarthritis: three dimensional assessment. Int. Orthop. 38, 1191–1198.
Chan, W.P., Lang, P., Stevens, M.P., Sack, K., Majumdar, S., Stoller, D.W., Basch, C., Genant, H.K., 1991. Osteoarthritis of the knee: comparison of radiography, CT, and MR imaging to assess extent and severity. Am. J. Roentgenol. 157 (4), 799–806.
Chen, C., Ma, Y., Geng, B., Tan, X., Zhang, B., Kumar Jayswal, C., Shahidur Khan, M., Meng, H., Ding, N., Jiang, J., Wu, M., Wang, J., Xia, Y., 2016. Intercondylar notch stenosis of knee osteoarthritis and relationship between stenosis and osteoarthritis complicated with anterior cruciate ligament injury a study in MRI. Medicine 95 (17), 1–7.
Cootes, T.F., Cooper, D.H., Taylor, C.J., Graham, J., 1992. Trainable method of parametric shape description. Image Vis. Comput. 10 (5), 289–294.
Ding, C., Cicuttini, F., Jones, G., 2007. Tibial subchondral bone size and knee cartilage defects: relevance to knee osteoarthritis. Osteoarth. Cartil. 15, 479–486.
Dryden, I.L., Mardia, K.V., 1998. Statistical Shape Analysis. John Wiley & Sons.

Fairbank, T.J., 1948. Knee joint changes after meniscectomy. J. Bone Joint Surg. 30B (4), 664–670.
Foroughi, N., Smith, R., Vanwanseele, B., 2009. The association of external knee adduction moment with biomechanical variables in osteoarthritis: a systematic review. Knee 16 (5), 303–309.
Freeman, M.A.R., Pinskerova, V., 2005. The movement of the normal tibio-femoral joint. J. Biomech. 38 (2), 197–208.
Gower, J.C., 1975. Generalized procrustes analysis. Psychometrika 40 (1).
Grood, E.S., Suntay, W.J., 1983. A joint coordinate system for the clinical description of three-dimensional motions: application to the knee. J. Biomech. Eng. 105 (2), 136–144.
Haverkamp, D.J., Schiphof, D., Bierma-Zeinstra, S.M., Weinans, H., Waarsing, J.H., 2011. Variation in joint shape of osteoarthritic knees. Arth. Rheum. 63 (11), 3401–3407.
Heimann, T., Meinzer, H.-P., 2009. Statistical shape models for 3D medical image segmentation: a review. Med. Image Anal. 13 (4), 543–563.
Hudelmaier, M., Wirth, W., 2016. Differences in subchondral bone size after one year in osteoarthritic and healthy knees. Osteoarth. Cartil. 24, 623–630.
Hunter, D.J., Guermazi, A., Lo, G.H., Grainger, A.J., Conaghan, P.G., Boudreau, R.M., Roemer, F.W., 2011. Evolution of semi-quantitative whole joint assessment of knee OA: MOAKS (MRI Osteoarthritis Knee Score). Osteoarth. Cartil. 19, 990–1002.
Hunter, D.J., Guermazi, A., Roemer, F., Zhang, Y., Neogi, T., 2013. Structural correlates of pain in joints with osteoarthritis. Osteoarth. Cartil. 21, 1170–1178.
Isaacson, J., Brotto, M., 2014. Physiology of mechanotransduction: how do muscle and bone "talk" to one another? Clin. Rev. Bone Miner. Metabol. 12 (2), 77–85.
Kellgren, J.H., Lawrence, J.S., 1957. Radiological assessment of osteoarthrosis. Ann. Rheum Dis. 16.
Van Manen, M.D., Nace, J., Mont, M.A., 2012. Management of primary knee osteoarthritis and indications for total knee arthroplasty for general practitioners. J. Am. Osteop. Associat. 112 (11), 709–715.
Matsuda, S., Miura, H., Nagamine, R., Mawatari, T., Tokunaga, M., Nabeyama, R., Iwamoto, Y., 2004. Anatomical analysis of the femoral condyle in normal and osteoarthritic knees. J. Orthop. Res. 22 (1), 104–109.
Neogi, T., 2012. Clinical significance of bone changes in osteoarthritis. Ther. Adv. Musculoskeletal Dis. 4 (4), 259–267.
Neogi, T., Bowes, M.A., Niu, J., De Souza, K.M., Vincent, G.R., Goggins, J., Zhang, Y., Felson, D.T., 2013. Magnetic resonance imaging-based three-dimensional bone shape of the knee predicts onset of knee osteoarthritis: data from the osteoarthritis initiative. Arth. Rheum. 65 (8), 2048–2058.
Pavlova, A.V., Saunders, F.R., Muthuri, S.G., Gregory, J.S., Barr, R.J., Martin, K.R., Hardy, R.J., Cooper, R., Adams, J.E., Kuh, D., Aspden, R.M., 2017. Statistical shape modelling of hip and lumbar spine morphology and their relationship in the MRC National Survey of Health and Development. J. Anat. 231 (2), 248–259.
Pinskerova, V., Samuelson, K.M., Stammers, J., Maruthainar, K., Sosna, A., Freeman, M.A.R., 2009. The knee in full flexion: an anatomical study. J. Bone Joint Surg. – Brit. Vol. 91 (6), 830–834.
Sasho, T., Akagi, R., Tahara, M., Katsuragi, J., Nakagawa, R., Enomoto, T., Yusuke, S., Kimura, S., Yamaguchi, S., Watanabe, A., 2017. Osteophyte formation on medial wall of the intercondylar notch of femur is an early sign of osteoarthritic knee development using osteoarthritis initiative data. Osteoarth. Cartil. 25, S84.
Scarvell, J.M., Galvin, C.R., Perriman, D.M., Lynch, J.T., van Deursen, R.W.M., 2018. 'Kinematics of knees with osteoarthritis show reduced lateral femoral roll-back and maintain an adducted position. A systematic review of research using medical imaging. J. Biomech. 75, 108–122.
Schneider, M.T.Y., Zhang, J., Crisco, J.J., Weiss, A.-P.C., Ladd, A.L., Mithraratne, K., Nielsen, P., Besier, T., 2017. Trapeziometacarpal joint contact varies between men and women during three isometric functional tasks. Med. Eng. Phys. 50, 43–49.
Schneider, M., Zhang, J., Crisco, J.J., Weiss, A.P.C., Ladd, A.L., Nielsen, P., Besier, T., 2015. Men and women have similarly shaped carpometacarpal joint bones. J. Biomech. 48, 3420–3426.
Schneider, M., Zhang, J., Walker, C., Crisco, J., Weiss, A.-P., Ladd, A., Nielsen, P., Besier, T., 2018. Early morphologic changes in trapeziometacarpal joint bones with osteoarthritis. Osteoarth. Cartil. 26 (10), 1338–1344.
Shepstone, L., Rogers, J., Kirwan, J.R., Silverman, B.W., 2001. Shape of the intercondylar notch of the human femur: a comparison of osteoarthritic and non-osteoarthritic bones from a skeletal sample. Ann. Rheum. Dis. 60, 968–973.
Skou, S.T., Roos, E.M., Laursen, M.B., Rathleff, M.S., Arendt-Nielsen, L., Simonsen, O., Rasmussen, S., 2015. A randomized, controlled trial of total knee replacement. N. Engl. J. Med. 373 (17), 1597–1606.
Smoger, L.M., Fitzpatrick, C.K., Clary, C.W., Cyr, A.J., Maletsky, L.P., Rullkoetter, P.J., Laz, P.J., 2015. Statistical modeling to characterize relationships between knee anatomy and kinematics. J. Orthop. Res. 33 (11), 1620–1630.
Steultjens, M.P.M., Dekker, J., van Baar, M.E., Oostendorp, R.A.B., Bijlsma, J.W.J., 2000. Range of joint motion and disability in patients with osteoarthritis of the knee or hip. Rheumatology 39 (9), 955–961.
Thambyah, A., Goh, J.C.H., De, S. Das, 2005. Contact stresses in the knee joint in deep flexion. Med. Eng. Phys. 27 (4), 329–335.
Wang, Y., Wluka, A.E., Cicuttini, F.M., 2005. The determinants of change in tibial plateau bone area in osteoarthritic knees: a cohort study. Arth. Res. Ther. 7 (3), 687–693.
Wluka, A.E., Wang, Y., Davis, S.R., Cicuttini, F., 2005. Tibial plateau size is related to grade of joint space narrowing and osteophytes in healthy women and in women with osteoarthritis. Ann. Rheum. Dis. 64 (7), 1033–1037.
Yildirim, G., Walker, P.S., Sussman-Fort, J., Aggarwal, G., White, B., Klein, G.R., 2007. The contact locations in the knee during high flexion. Knee 14 (5), 379–384.
Zhang, J., Ackland, D., Fernandez, J., 2018. Point-cloud registration using adaptive radial basis functions. Comput. Methods Biomech. Biomed. Eng. 21 (7), 498–502.
Zhang, J., Malcolm, D., Hislop-Jambrich, J., Thomas, C.D.L., Nielsen, P.M.F., 2014. An anatomical region-based statistical shape model of the human femur. Comput. Methods Biomech. Biomed. Eng.: Imaging Visual. 2 (3), 176–185.